Kırklareli Üniversitesi
Mühendislik ve Fen Bilimleri Dergisi
Cilt 11, Sayı 2, 253-266, 2025

Kırklareli University
Journal of Engineering and Science
Volume 11 Issue 2, 253-266, 2025

Research Article

DOI: 10.34186/klujes.1804214

IoU-Based Anchor Box Estimation for Enhanced Lung Region Localization in Chest X-rays Using YOLO v4

Serdar Abut[1*]

[1]*Department of Artificial Intelligence and Machine Learning, Kayseri University, Kayseri, Türkiye*

Received: 15.10.2025, Accepted: 08.12.2025, Published: 20.12.2025

ABSTRACT

Precise lung region detection in chest radiographs is an essential preprocessing step for computer-aided diagnostics. This study presents a YOLO v4–based framework to automatically localize lung regions in posteroanterior (PA) chest X-rays. A subset of the CheXpert dataset, containing 456 manually annotated PA radiographs, was used. Anchor boxes were estimated via an Intersection-over-Union (IoU)–based clustering method, improving scale invariance and shape alignment over Euclidean metrics. Empirical evaluation showed that six anchor boxes achieved the best balance between mean IoU (0.883) and computational efficiency. The trained model was tested on 144 images, yielding Average Precision (AP) of 0.9043 for the lung_region class, which represents only the anatomical lung area and not any specific pathology. The precision–recall curve indicated high precision across most recall values, and the confusion matrix showed 124 true positives, 13 false positives, and 7 false negatives. These results demonstrate that YOLO v4 with optimized anchor box estimation enables accurate, efficient lung region localization, supporting automated radiology workflows.

Keywords: Lung Region Detection; Image Processing; YOLO v4; Anchor Box Optimization; Object Detection

YOLO v4 Kullanarak Göğüs Röntgenlerinde Geliştirilmiş Akciğer Bölgesi Yerelleştirme için IoU Tabanlı Çapa Kutusu Tahmini

ÖZ

Göğüs röntgenlerinde akciğer bölgesinin doğru tespiti, bilgisayar destekli tanı sistemleri için kritik bir ön işleme adımıdır. Bu çalışmada, posteroanterior (PA) göğüs röntgenlerinde akciğer bölgelerini otomatik olarak yerelleştirmek için YOLO v4 tabanlı bir çerçeve sunulmuştur. CheXpert veri kümesinden 456 adet elle anotlanmış PA röntgen kullanılmıştır. Çapa kutuları, ölçekten bağımsız mesafe ölçümü ve şekil hizalamasında iyileşme sağlayan IoU (Intersection-over-Union) tabanlı kümeleme yöntemiyle tahmin edilmiştir. Deneysel değerlendirmeler, altı çapa kutusunun ortalama IoU (0,883) ve hesaplama verimliliği açısından en iyi dengeyi sunduğunu göstermiştir. Eğitilen model, 144 görüntüden oluşan test kümesinde çalıştırılmış ve lung_region sınıfı, yalnızca anatomik akciğer bölgesini temsil etmekte olup herhangi bir patolojiyi göstermemektedir; Doğruluk (AP) değeri 0,9043 elde edilmiştir. Kesinlik–duyarlılık eğrisi, çoğu duyarlılık değerinde yüksek kesinlik göstermiştir. Karmaşıklık matrisi ise 124 doğru pozitif, 13 yanlış pozitif ve 7 yanlış negatif tespit etmiştir. Sonuçlar, optimize edilmiş çapa kutusu tahmini ile YOLO v4'ün doğru ve verimli akciğer bölgesi yerelleştirmesi sağlayabildiğini göstermektedir.

Anahtar Kelimeler: Akciğer Bölgesi Tespiti; Görüntü İşleme; YOLO v4; Çapa Kutusu Optimizasyonu; Nesne Tespiti

*Corresponding Author: Serdar Abut
E-mail: *serdarabut@kayseri.edu.tr*

1. INTRODUCTION

The increasing use of Artificial Intelligence (AI) in the medical domain, particularly in medical image analysis, has been propelled by a paradigm shift from traditional Artificial Neural Networks (ANNs) to deep Convolutional Neural Networks (DCNNs) (Abut et al., 2024). These models have shown remarkable performance in tasks such as disease classification from chest X-rays, facial image-based gender recognition (Ergen & Abut, 2013), and broader applications in medical decision-making (Abut & Okut, 2024). Despite these successes, explainability and reliability remain critical challenges. A promising solution is to apply segmentation techniques to isolate the lung region prior to classification. By enforcing the model to learn only from relevant anatomical structures, segmentation improves both accuracy and interpretability. For example, COPD-GradeNet is a model proposal that integrates lung-region-focused learning to predict the severity of chronic obstructive pulmonary disease (COPD) (Abut, 2024).

Recent studies emphasize the importance of considering anatomical structures in medical imaging. This attention spans multiple domains, including nuclear marker quantification in tumor tissues (Yilmaz et al., 2025b), AI-based segmentation of kidney biopsies (Yilmaz et al., 2025a; Yilmaz et al. 2025c), and emergency care applications (Berikol et al., 2025). These approaches collectively underline the importance of guiding AI models toward relevant visual features to improve diagnostic reliability.

Although deep learning-based models have shown promising results in the classification of lung diseases, careful visual analyses are required to explain their decision-making processes and improve their accuracy. Visualization techniques such as Grad-CAM make it possible to analyze which regions the model focuses on when making decisions. As shown in Figure 1, the classification model focused not on the lung image itself but on irrelevant areas in the corner of the image. Such deviations indicate that the model may lead to incorrect generalizations and pose reliability issues. In this context, applying lung region segmentation to ensure that the model considers only the relevant anatomical areas (e.g., lung lobes) during decision-making is of critical importance. Performing segmentation as a preprocessing step helps guide the model's attention to the correct region and improves classification performance (Irvin et al., 2019; Rajpurkar et al., 2017).

Figure 1: Grad-CAM visualization applied to a chest X-ray image

In Figure 1, the left image shows the attention map overlaid on the original X-ray, where red areas indicate higher attention weights of the model. It can be observed that the classifier has focused on irrelevant regions such as the top-left corner of the image rather than the lung area, which is the anatomically meaningful region for diagnosis. This highlights the necessity of restricting the model's attention to the lung region via segmentation-based preprocessing for more accurate disease classification.

Recent advances in deep learning, particularly convolutional neural networks (CNNs), have revolutionized medical image analysis by enabling hierarchical feature learning directly from raw data, leading to improved accuracy in various tasks including classification, segmentation, and localization of diseases in CXR images. Deep learning models have demonstrated superior performance in detecting lung infections, cancers, and other thoracic abnormalities by effectively learning spatial-contextual patterns that are not readily captured by traditional approaches.

Given the importance of correctly identifying the lung region to reduce irrelevant information and improve model performance, this study employs a YOLOv4-based deep learning framework for automatic localization and rectangular cropping of lung areas in posteroanterior chest X-rays. Unlike methods that perform precise boundary segmentation, the proposed approach focuses on bounding-box localization rather than pixel-level delineation, thereby preserving peripheral contextual cues that may contribute to disease classification. This design choice also prevents potential loss of diagnostically relevant patterns beyond the strict anatomical lung borders.

Prior studies have explored various segmentation techniques, including texture-based filtering combined with morphological operations to generate lung masks, which successfully excluded non-lung areas such as the shoulder and diaphragm regions (Matsuyama, 2021). Other research leveraged deep CNN architectures

like DenseNet-121 with transfer learning to classify lung nodules and cancer from chest X-rays, highlighting the role of precise lung region localization in improving diagnostic accuracy (Ausawalaithong et al., 2018). More recent work has integrated segmentation and classification networks, combining encoder-decoder frameworks such as UNet++ with classification modules, achieving high precision in lung infection localization and disease detection with efficient model designs suitable for clinical applications (Miah et al., 2024).

Moreover, deep Siamese networks have been employed to compare symmetrical lung segments for pneumonia classification, illustrating the utility of lung segmentation as a preprocessing step for enhanced disease detection (Acharya & Satapathy, 2020). Surveys and reviews indicate a growing trend toward leveraging advanced deep learning models for diverse chest X-ray analysis tasks, emphasizing the need for robust lung localization to support downstream applications (Ait Nasser & Akhloufi, 2023; Çallı et al., 2021).

In this context, the present study introduces an automated deep learning pipeline focusing on accurate lung region detection and bounding box–based cropping in chest X-rays, intended to facilitate and improve the performance of various CAD systems for thoracic disease diagnosis. While object detection networks such as YOLO have been widely adopted in natural image analysis, their systematic application for lung region localization within MATLAB-based medical imaging workflows has been limited. This study addresses this practical gap by implementing and optimizing YOLOv4 for robust, efficient localization of lung fields, mitigating the confounding influence of non-anatomical artifacts (e.g., labels or external patterns) commonly present in chest radiographs. The resulting framework offers a reproducible preprocessing solution that enhances downstream diagnostic modeling by providing clean, context-preserving input regions.

2. MATERIAL AND METHOD

2.1. Dataset

In this study, a subset of the publicly available CheXpert dataset (Saporta et al., 2022) was utilized to develop and evaluate the lung localization framework. Only posteroanterior (PA) view radiographs were included to maintain consistency in image orientation and diagnostic relevance, while lateral views were excluded. From the CheXpert collection, 456 images were selected based on the presence of clear lung regions and sufficient image quality, following a semi-random sampling procedure that ensured diversity across different thoracic pathologies. This subset was primarily used for lung region localization; a related

but distinct study is being conducted to investigate Atelectasis classification using the same source dataset but with a different methodological focus.

2.2. Manual Annotation

Prior to training the YOLO model, each of the 456 selected chest radiographs underwent manual annotation to identify the lung regions. Manual annotation of lung regions was carried out to generate the ground-truth bounding boxes used for training and evaluation. Each chest X-ray was visually inspected, and the lung boundaries were marked to define the minimal rectangular area covering both lungs. The manual annotations were performed by a biomedical engineer experienced in medical image processing, following consistent visual criteria to ensure reproducibility and minimize subjectivity across all samples. Figure 2 illustrates an example of the annotated regions used in the experiments. A rectangular bounding box was drawn around the visible lung fields in each image, ensuring that the entire lung area was enclosed within the frame. The corner coordinates (top-left and bottom-right) of each bounding box were manually recorded for every image. These coordinates served as ground truth data for the subsequent training of the object detection model (Figure 2).

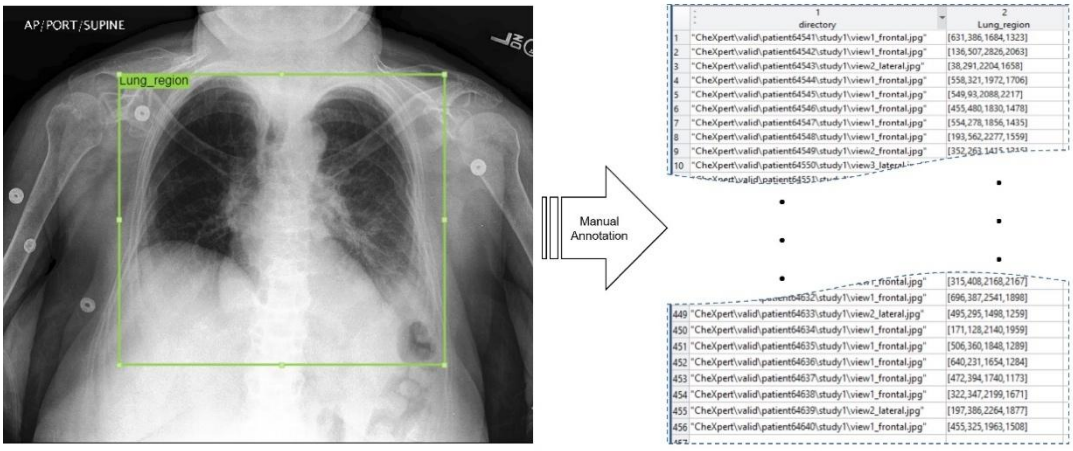

Figure 2: Manual annotation of the lung region

2.3. Implementation of YOLO v4 for Object Detection and Anchor Box Estimation

In this study, the YOLO v4 object detection network was utilized for lung region detection. YOLO v4 is a one-stage object detector that provides a balanced trade-off between detection speed and accuracy (Bochkovskiy et al., 2020).

During model training, the input image size was fixed at 416×416 pixels. Based on the locations and sizes of lung regions in the training data, suitable predefined anchor boxes were estimated. The YOLOv4 model was trained using the Adam optimizer with gradient decay factors of 0.9 and 0.999, an initial learning rate of 0.001, and an L2 regularization factor of 0.0005. The training was performed for 80 epochs with a mini-

batch size of 4, and the best-performing model was selected based on the lowest validation loss. Training and validation data were shuffled at each epoch to prevent overfitting, and checkpointing was applied to save intermediate models. The total training process was completed in approximately 45 minutes.

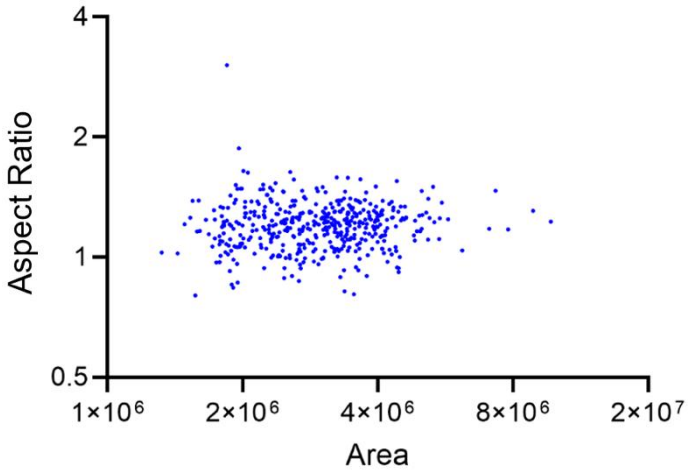

Figure 3: Distribution of anchor box areas (in pixels) with respect to their aspect ratios

Figure 3 shows the distribution of aspect ratios of the manually annotated rectangles during training, plotted against their corresponding areas within the images. It can be observed from the figure that the distribution appears approximately uniform on average. Anchor boxes were estimated from the training data using a method based on the intersection-over-union (IoU) distance metric (Figure 4). The reason for using an IoU-based distance metric is its invariance to box sizes, unlike the Euclidean distance metric, which tends to produce larger errors as box dimensions increase (Redmon & Farhadi, 2017). In addition, it was considered that the IoU metric would cause boxes corresponding to the lung region—generally having similar aspect ratios and sizes across the images—to be clustered together, thus resulting in anchor boxes that better fit the data.

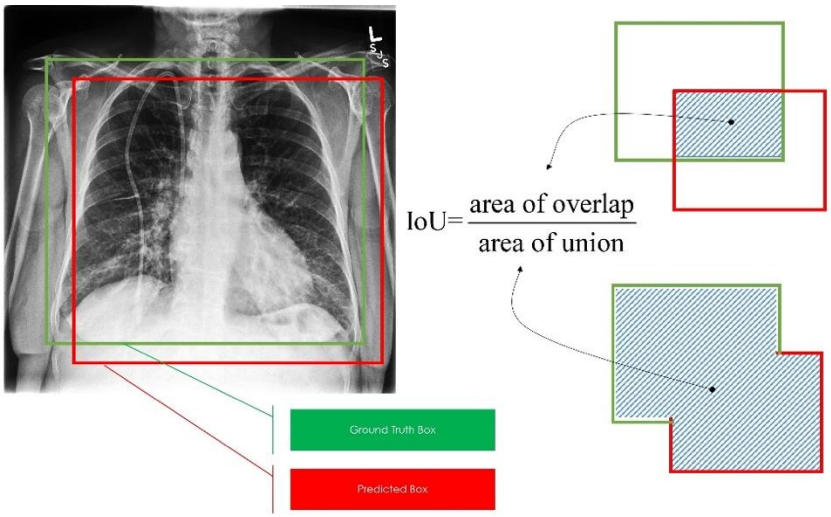

Figure 4: Mean IoU values obtained by using different numbers of anchor boxes.

A mean IoU value of approximately 0.83 is achieved using two anchor boxes, and the mean IoU is improved up to about 0.88 by increasing the number of anchor boxes to six. Beyond six anchor boxes, only marginal improvements in mean IoU are observed. Given these results, multiple object detectors are planned to be trained and evaluated using anchor box counts between 2 and 6. This empirical analysis is conducted to determine the optimal number of anchor boxes required to balance detection accuracy and computational efficiency. The IoU value improves significantly up to 6 anchor boxes (0.883), after which the gains become marginal (Figure 5). Based on this, 6 anchor boxes were selected as a balance between performance and model complexity for further training and evaluation.

Six anchor boxes were estimated and sorted in descending order based on their areas. Thus, larger anchor boxes were assigned to lower-dimensional feature map layers of the network, while smaller anchor boxes were assigned to higher-dimensional feature map layers. This approach enabled more effective detection of lung regions at different scales.

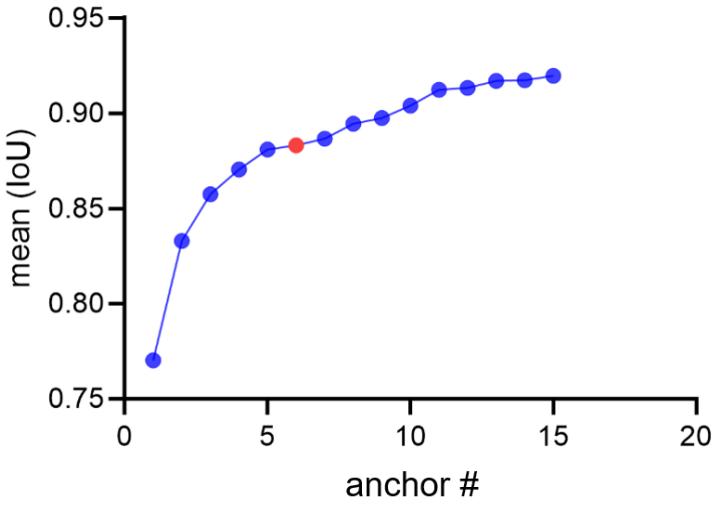

Figure 5: Mean IoU values obtained by using different numbers of anchor boxes.

2.4. Evaluation Metric (Average Precision)

For performance evaluation, the Average Precision (AP) metric was employed since the model detects a single class (lung_region). The AP was computed at an Intersection-over-Union (IoU) threshold of 0.5, corresponding to the conventional mAP@0.5 criterion used in object detection tasks. This threshold ensures that the predicted bounding boxes have at least 50% overlap with the ground-truth annotations, which is considered sufficient for reliable localization. Additionally, the mean IoU between predicted and annotated boxes was analyzed as a complementary measure to assess the spatial alignment quality. The relationship between the number of anchor boxes and the mean IoU was also examined to balance detection accuracy and computational efficiency.

Regardless of the interpolation strategy employed, the Average Precision (AP) is calculated separately for each object class. In datasets containing a large number of classes, it is often desirable to summarize detection performance with a single, representative metric.

3. RESULTS AND DISCUSSIONS

3.1. Results

The performance of the trained object detection model was evaluated using a dedicated test set consisting of 144 chest X-ray images. It should be noted that the test dataset consists of 144 images, which constitutes a relatively small sample. While the results demonstrate promising lung region detection performance, larger-scale evaluation on diverse datasets would be necessary to fully validate the generalizability of the method. The evaluation focused on assessing the model's ability to accurately detect the lung_region class.

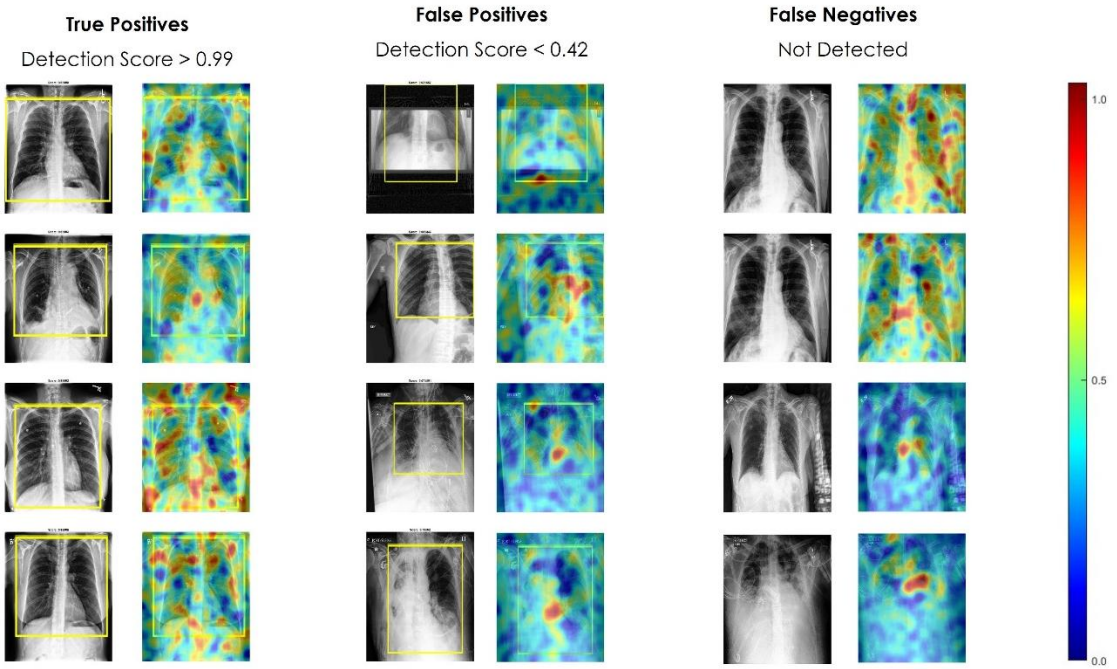

Figure 6: Representative detection outcomes from the test set with Grad-CAM visualizations using the D-RISE method (Petsiuk et al., 2021):True positive, false positive, and false negative cases are shown; detailed column descriptions are provided in the main text.

It should be clarified that the detected single class, lung_region, does not correspond to a pathology. The aim is to isolate the lung area in chest X-rays to reduce irrelevant information and improve model attention, rather than to detect diseases. Hence, the single-class detection serves as a preprocessing step for downstream tasks and does not limit the framework's potential applicability to disease detection with additional data.

Figure 6 illustrates representative detection outcomes from the test set, complemented by Grad-CAM visualizations generated using the D-RISE method (Petsiuk et al., 2021). The first column shows true positive cases where the lung region is correctly detected by the model. The second column presents false positive cases in which non-lung areas were mistakenly identified as lung regions. The third column displays false negative cases, where actual lung regions were present but not detected by the model. This breakdown highlights both the strengths and limitations of the YOLOv4-based localization approach.

A low detection threshold of 0.01 was used during inference to ensure that a broad range of detections could be captured. This strategy facilitated the analysis of the model's precision over a wide spectrum of recall values, thereby enabling a more comprehensive performance characterization.

The evaluation was conducted based on the average precision (AP) metric, which integrates both the ability of the model to correctly classify detected objects (precision) and its ability to retrieve all relevant instances (recall). The computed AP value for the lung_region class was 0.9043, indicating that the detector achieved high precision while maintaining a substantial level of recall (Figure 7).

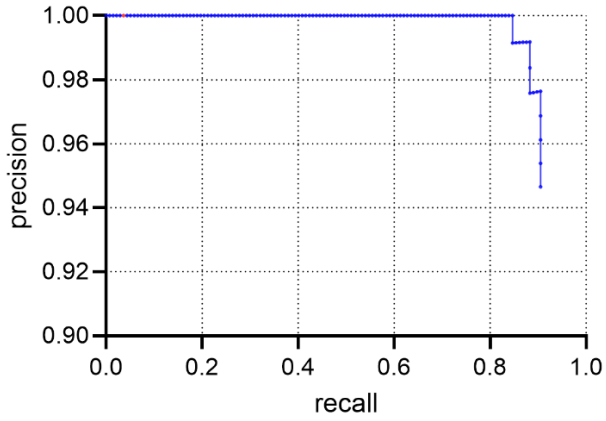

Figure 7: Precision–recall (PR) curve for the lung_region class obtained from the test dataset.

The corresponding precision-recall (PR) curve, shown in Figure 7, revealed that precision remained consistently at 1.0 throughout a large portion of the recall range, with a gradual decline observed only at higher recall levels. This behavior suggests that the model was able to detect most of the relevant lung regions without introducing a significant number of false positives.

Figure 6 presents representative detection outcomes from the test set, along with Grad-CAM visualizations generated using the D-RISE method (Petsiuk et al., 2021). In the true positive cases (left column), the YOLO v4 model achieved high detection scores (> 0.99) and the activation maps show strong spatial correspondence between high-intensity regions and the annotated lung fields, indicating that the network effectively focused on relevant anatomical structures. In contrast, false positives (middle column) primarily

occurred when non-lung anatomical regions such as the clavicle, shoulder, or mediastinal area were misclassified as lung regions. The associated Grad-CAM maps reveal attention leakage toward surrounding high-contrast structures, often outside the intended lung boundaries. False negatives (right column) illustrate instances where lung regions were present but not detected; although activation maps occasionally showed partial focus on the lungs, this attention was insufficient to trigger a detection output. These failure cases suggest potential improvements through enhanced anchor box tuning, inclusion of more challenging training examples, and augmentation strategies that increase robustness to anatomical variability and low-contrast imaging conditions.

Overall, the D-RISE visualizations provide valuable insight into the model's decision-making process, highlighting both strengths in accurate lung localization and limitations leading to missed or spurious detections.

In addition, a confusion matrix in Equation (1) was generated to provide further insight into the classification performance. As shown below, the model produced 124 true positives, 13 false positives, 7 false negatives, and 0 true negatives:

$$\begin{bmatrix} \text{TP} & \text{FN} \\ \text{FP} & \text{TN} \end{bmatrix} = \begin{bmatrix} 124 & 7 \\ 13 & 0 \end{bmatrix} \tag{1}$$

This matrix confirms the high sensitivity of the detector, although it also highlights a modest false positive rate. Nevertheless, given the high AP score and the favorable shape of the PR curve, it can be concluded that the model performs reliably in detecting lung regions in chest X-ray images.

Based on these results, the lung region was correctly detected in 124 out of the 144 images in the test group. In 7 cases, an area outside the actual lung region was incorrectly detected as a lung region, while in 13 chest X-ray images, the detector failed to identify a region despite the presence of an actual lung region. Figure 6 presents five representative examples each of true positives, false positives, and false negatives.

In comparison to previous works using YOLO-based object detection in chest imaging, our approach focuses specifically on bounding-box localization and cropping of the lung region rather than pathology classification. For instance, Detection Method of Chest X-ray Lung Nodules Based on Improved YOLOv3 Model(Yan, 2020) used an improved YOLOv3 architecture to detect lung nodules on chest X-rays and reported a detection accuracy of approximately 61% on nodules.

Meanwhile, Anomalies Detection in Chest X-Ray Images Using Faster R-CNN and YOLO (2025) applied YOLOv5s to identify five different thoracic abnormalities and reported AP@0.5 and AP@[0.5:0.95] values of roughly 0.616 and 0.322 respectively on 2,500 X-ray images (Nguyen et al., 2023).

By contrast, our method achieves a mean IoU of 0.883 and an AP of 0.9043 for the lung_region class in a 144-image test set. Although direct comparisons are limited due to differing tasks and datasets, the strong localization performance of our method suggests that bounding-box cropping of the lung region may provide a robust preprocessing step for downstream diagnostic models.

3.2. Discussion

Accurate localization of lung regions is a critical prerequisite for computer-aided diagnosis (CAD) systems targeting thoracic pathologies such as Atelectasis, Cardiomegaly, and Pleural Effusion. In this study, YOLO v4 was selected due to its proven balance between detection speed and accuracy, aligning with prior evaluations demonstrating its superior real-time performance even on moderate GPUs % (Bochkovskiy et al., 2020) and other benchmarks in medical contexts (Ragab et al., 2024).

The relatively small size of the test dataset may limit the generalizability of the model and increase the risk of overfitting. Future studies with larger and more diverse datasets are needed to validate and further improve the robustness of the proposed approach.

Future work could explore strategies to further enhance model robustness and generalizability. Approaches such as data augmentation, transfer learning, and domain adaptation may help address the limitations imposed by the relatively small dataset, reduce overfitting, and improve performance across diverse patient populations and imaging conditions. Implementing these techniques could facilitate the extension of the current framework to multi-class detection tasks and broader clinical applications.

The high AP score (0.9043) and the PR curve characteristics suggest that the proposed model can reliably detect lung regions in chest X-rays while maintaining low false-positive rates. The IoU-based anchor box estimation played a pivotal role in optimizing detection accuracy (Redmon & Farhadi, 2016), consistent with prior reports that IoU-based clustering outperforms Euclidean distance for object detection tasks in medical imaging (Redmon & Farhadi, 2016). Despite the encouraging results, some false positives and false negatives were observed. The false positives often occurred in regions adjacent to the diaphragm or mediastinum, potentially due to overlapping soft tissue densities. False negatives were mainly associated with atypical lung shapes or reduced contrast in diseased lungs, highlighting a limitation in model generalization to highly variable anatomical presentations.

IoU-based anchor box optimization helps the model focus on actual lung regions by excluding irrelevant areas such as image borders or markers. These non-lung regions can distract deep networks, so aligning anchors with lung fields reduces such noise and conceptually improves feature learning and downstream performance.

Future research should address these limitations by integrating contrast enhancement techniques, multi-view learning, and domain adaptation to handle variations across datasets. Additionally, incorporating explainability methods such as Grad-CAM could aid in model interpretability, thereby increasing clinician trust in AI-assisted diagnostic workflows (Han et al., 2022; Holzinger et al., 2020)

The Grad-CAM and D-RISE visualizations provide insights into the regions of the chest X-rays that the model focuses on during lung region detection, enhancing the clinical interpretability of the results. In this study, we plan to incorporate these visualizations in ablation experiments to systematically evaluate how excluding or modifying certain image regions affects model attention and performance. This approach will help demonstrate the reliability of the model's focus and support the interpretability of automated detection outcomes.

4. CONCLUSION

This study demonstrated that YOLO v4, combined with IoU-based anchor box optimization, provides an effective and computationally efficient solution for lung region detection in chest X-ray images. Using six optimized anchor boxes yielded a high AP score of 0.9043 and robust detection performance across the test set, confirming the suitability of this approach for clinical pre-processing tasks in computer-aided diagnosis (Bochkovskiy et al., 2020; Redmon & Farhadi, 2017).

The accurate identification of lung regions facilitates subsequent diagnostic tasks, including the detection and classification of Atelectasis and other thoracic pathologies. While some false positives and false negatives persist, these can be mitigated through enhanced preprocessing, increased dataset diversity, and the integration of advanced explainability techniques (Bochkovskiy et al., 2020; Holzinger et al., 2020; Redmon & Farhadi, 2016).

Given its strong performance and scalability, the proposed method holds significant potential for deployment in automated radiology pipelines, improving workflow efficiency and diagnostic consistency in clinical settings.

DATA AVAILABILITY

The MATLAB implementation of the YOLOv4-based lung region detection framework, including functions for annotation and cropping, is publicly available at:

- https://www.mathworks.com/matlabcentral/fileexchange/182683-chestx-lungcrop

CONFLICT OF INTEREST STATEMENT

There is no conflict of interest among the authors.

REFERENCES

Abut, S. (2024). AI-based model design for prediction of COPD grade from chest X-ray images: a model proposal (COPD-GradeNet). *Cukurova University Journal of the Faculty of Engineering*, *39*(2), 325-338.

Abut, S., & Okut, H. (2024). The Importance of Artificial Neural Networks in Decision Making for the Field of Medicine. In G. A. Indrajit, Mittal; Hemlata, Jain (Ed.), *The Future of Artificial Neural Networks* (pp. 1-24). Nova Science. https://doi.org/10.52305/YUZX7201

Abut, S., Okut, H., & Kallail, K. J. (2024). Paradigm shift from Artificial Neural Networks (ANNs) to deep Convolutional Neural Networks (DCNNs) in the field of medical image processing. *Expert Systems with Applications*, *244*, 122983.

Acharya, A. K., & Satapathy, R. (2020). A deep learning based approach towards the automatic diagnosis of pneumonia from chest radio-graphs. *Biomedical and Pharmacology Journal*, *13*(1), 449-455.

Ait Nasser, A., & Akhloufi, M. A. (2023). A review of recent advances in deep learning models for chest disease detection using radiography. *Diagnostics*, *13*(1), 159.

Ausawalaithong, W., Thirach, A., Marukatat, S., & Wilaiprasitporn, T. (2018, 21-24 Nov. 2018). Automatic Lung Cancer Prediction from Chest X-ray Images Using the Deep Learning Approach. 2018 11th Biomedical Engineering International Conference (BMEiCON),

Berikol, G. B., Kanbakan, A., Ilhan, B., & Doğanay, F. (2025). Mapping artificial intelligence models in emergency medicine: A scoping review on artificial intelligence performance in emergency care and education. Turkish Journal of Emergency Medicine, 25(2), 67-91.

Bochkovskiy, A., Wang, C.-Y., & Liao, H.-Y. M. (2020). Yolov4: Optimal speed and accuracy of object detection. *arXiv preprint arXiv:2004.10934*.

Çallı, E., Sogancioglu, E., Van Ginneken, B., van Leeuwen, K. G., & Murphy, K. (2021). Deep learning for chest X-ray analysis: A survey. *Medical image analysis*, *72*, 102125.

Ergen, B., & Abut, S. (2013). Gender recognition using facial images. *International Proceedings of Chemical, Biological & Environmental Engineering*, *60*(22), 112-117. https://doi.org/10.7763/IPCBEE.2013.V60.22

Han, Y., Chen, C., Tewfik, A., Glicksberg, B., Ding, Y., Peng, Y., & Wang, Z. (2022). Knowledge-augmented contrastive learning for abnormality classification and localization in chest X-rays with radiomics using a feedback loop. Proceedings of the IEEE/CVF winter conference on applications of computer vision,

Holzinger, A., Saranti, A., Molnar, C., Biecek, P., & Samek, W. (2020). Explainable AI methods-a brief overview. International workshop on extending explainable AI beyond deep models and classifiers,

Irvin, J., Rajpurkar, P., Ko, M., Yu, Y., Ciurea-Ilcus, S., Chute, C., Marklund, H., Haghgoo, B., Ball, R., & Shpanskaya, K. (2019). Chexpert: A large chest radiograph dataset with uncertainty labels and expert comparison. Proceedings of the AAAI conference on artificial intelligence,

Matsuyama, E. (2021). A novel method for automated lung region segmentation in chest X-ray images. *Journal of biomedical science and engineering*, *14*(6), 288-299.

Miah, M. A. I., Paul, S., Das, S., & Hashem, M. (2024). Inflocnet: Enhanced lung infection localization and disease detection from chest x-ray images using lightweight deep learning. *arXiv preprint arXiv:2408.06459*.

Nguyen, H. T., Nguyen, M. N., Phung, L. D., & Pham, L. T. T. (2023). Anomalies Detection in Chest X-Rays Images Using Faster R-CNN and YOLO. *Vietnam Journal of Computer Science*, *10*(04), 499-515. https://doi.org/10.1142/s2196888823500094

Petsiuk, V., Jain, R., Manjunatha, V., Morariu, V. I., Mehra, A., Ordonez, V., & Saenko, K. (2021). Black-box explanation of object detectors via saliency maps. Proceedings of the IEEE/CVF conference on computer vision and pattern recognition,

Ragab, M., Jadid Abdulkadir, S., Muneer, A., Alqushaibi, A., Sumiea, E., Qureshi, R., Al-Selwi, S., & Alhussian, H. (2024). A Comprehensive Systematic Review of YOLO for Medical Object Detection (2018 to 2023). *IEEE Access*, *PP*, 1-1. https://doi.org/10.1109/ACCESS.2024.3386826

Rajpurkar, P., Irvin, J., Zhu, K., Yang, B., Mehta, H., Duan, T., Ding, D., Bagul, A., Langlotz, C., & Shpanskaya, K. (2017). Chexnet: Radiologist-level pneumonia detection on chest x-rays with deep learning. *arXiv preprint arXiv:1711.05225*.

Redmon, J., & Farhadi, A. (2016). YOLO9000: Better, Faster, Stronger. *2017 IEEE Conference on Computer Vision and Pattern Recognition (CVPR)*, 6517-6525.

Redmon, J., & Farhadi, A. (2017). YOLO9000: better, faster, stronger. Proceedings of the IEEE conference on computer vision and pattern recognition,

Saporta, A., Gui, X., Agrawal, A., Pareek, A., Truong, S. Q. H., Nguyen, C. D. T., Ngo, V.-D., Seekins, J., Blankenberg, F. G., Ng, A. Y., Lungren, M. P., & Rajpurkar, P. (2022). Benchmarking saliency methods for chest X-ray interpretation. *Nature Machine Intelligence*, *4*(10), 867-878. https://doi.org/10.1038/s42256-022-00536-x

Yan, S. (2020). Detection Method of Chest X-ray Lung Nodules Based on Improved YOLOV3 Model. *Science Discovery*, *8*(1), 18-23. https://doi.org/10.11648/j.sd.20200801.15

Yilmaz, I., Alazab, H., Doganay, F., Dangott, B., Albadri, S., Nassar, A., . . . Salem, F. (2025). 1492 SegRenal: AI-Powered Segmentation and Quantification of Frozen Section Histopathology of Preimplantation Kidney Biopsies. Laboratory Investigation, 105(3). doi:10.1016/j.labinv.2024.103732

Yilmaz, I., Alazab, H., Doganay, F., Dangott, B., Nassar, A., & Akkus, Z. (2025). 1398 AI-Powered Detection and Quantification of General-Purpose Nuclear Marker in Immunohistochemically Stained Tumor Tissues. Laboratory Investigation, 105(3).

Yilmaz, I., Alazab, H. M., Doganay, F., Dangott, B., Albadri, S., Nassar, A., . . . Akkus, Z. SegRenal: AI-Driven Segmentation of Frozen Sections in Transplant Kidney Biopsies-A Comparative Analysis of Deep Learning Models. Authorea Preprints.